separations

MDPI

Article

Fractions of Methanol Extracts from the Resurrection Plant *Haberlea rhodopensis* Have Anti-Breast Cancer Effects in Model Cell Systems

Diana Zasheva [1,*], Petko Mladenov [2], Krasimir Rusanov [2], Svetlana Simova [3], Silvina Zapryanova [1], Lyudmila Simova-Stoilova [4], Daniela Moyankova [2] and Dimitar Djilianov [2]

[1] Institute of Biology and Immunology of Reproduction, Bulgarian Academy of Sciences, Tsarigradsko Shosse, 73, 1113 Sofia, Bulgaria; silvina_z@abv.bg
[2] Agrobioinstitute, Agricultural Academy, 1164 Sofia, Bulgaria; mladenovpetko@yahoo.com (P.M.); krusanov@abv.bg (K.R.); dmoyankova@abi.bg (D.M.); d_djilianov@abi.bg (D.D.)
[3] Institute of Organic Chemistry with Centre of Phytochemistry (IOCCP), Bulgarian Academy of Sciences, 1113 Sofia, Bulgaria; svetlana.simova@orgchm.bas.bg
[4] Institute of Plant Physiology and Genetics, Bulgarian Academy of Science, 1113 Sofia, Bulgaria; lpsimova@yahoo.co.uk
* Correspondence: zasheva.diana@yahoo.com

Abstract: Breast cancer is among the most problematic diseases and a leading cause of death in women. The methods of therapy widely used, so far, are often with many side effects, seriously hampering patients' quality of life. To overcome these constraints, new cancer treatment alternatives are constantly tested, including bioactive compounds of plant origin. Our aim was to study the effects of *Haberlea rhodopensis* methanol extract fractions on cell viability and proliferation of two model breast cancer cell lines with different characteristics. In addition to the strong reduction in cell viability, two of the fractions showed significant influence on the proliferation rate of the hormone receptor expressing MCF7 and the triple negative MDA-MB231 breast cancer cell lines. No significant effects on the benign MCF10A cell line were observed. We applied a large scale non-targeted approach to purify and identify highly abundant compounds from the active fractions of *H. rhodopensis* extracts. By the combined NMR/MS approach, myconoside was identified in the fractions and hispidulin 8-C-(6-O-acetyl-2″-O-syringoyl-β-glucopyranoside) was found in one of them. We further performed molecular docking analysis of possible myconoside interactions with several proteins, important for breast cancer proliferation. High probability of binding was established for GLUT1 transporter, estrogen receptor and MYST acetyltransferase. Our results are a good background for future studies on the use of myconoside for targeted breast cancer therapy.

Keywords: breast cancer; *Haberlea rhodopensis*; myconoside; hispidulin 8-C-(6-O-acetyl-2″-O-syringoyl-β-glucopyranoside); GLUT1 transporter; estrogen receptor and MYST acetyltransferase

Citation: Zasheva, D.; Mladenov, P.; Rusanov, K.; Simova, S.; Zapryanova, S.; Simova-Stoilova, L.; Moyankova, D.; Djilianov, D. Fractions of Methanol Extracts from the Resurrection Plant *Haberlea rhodopensis* Have Anti-Breast Cancer Effects in Model Cell Systems. *Separations* **2023**, *10*, 388. https://doi.org/10.3390/separations10070388

Academic Editor: Faiyaz Shakeel

Received: 6 June 2023
Revised: 27 June 2023
Accepted: 28 June 2023
Published: 1 July 2023

1. Introduction

One of the most problematic diseases related to women's health is breast cancer. Cases of breast cancer diagnosed in 2008 were 1.38 million [1] and their number increased to 2.3 million in 2020 [2], thus reaching 12% of all cancer cases [3]. At the same time, breast cancer is the second leading cause of death in women [4]. The first step in finding new anticancer substances is to test them on model cell lines that have features common to different types of cancer. Cell cultures remain indispensable tools in cancer research, despite some limitations due to phenotypic drifts, some heterogeneity and existence of clonal variants. The cellular characteristics of breast cancer and the changes in their cell signal pathways complicate the therapeutic methods used so far. Invasive cancer types, named basal, are characterized with low expression of HER (Human Epidermal Growth

Factor Receptor) and a loss of estrogen and progesterone receptors [5]. They are also known as triple negative and are unresponsive of hormonal replacement therapy. A good model system to study new anticancer agents suitable for this very aggressive type of cancer is the cell line MDA-MB231 [6]. The expression of HER2 receptor and two hormonal receptors (estrogen and progesterone ones) characterizes luminal B types of breast cancer, known also as triple positive. A widely used model system of the hormone receptor expressing cancer is the cell line MCF7 [4]. This cell line is also used to study epigenetic regulation of cancer growth, mediated by higher expression and activity of MYST acetyltransferases in estrogen dependent breast tumors [7]. Several breast cancer cell lines, including MDA-MB231 and MCF7, are characterized with high rates of glucose uptake and high expression of glucose transporters of the GLUT family [6], which is not typical for noncancerous epithelial cell lines such as MCF-10A.

Conventionally used therapeutic methods are invasive and with many side effects. Often, the standardly used chemotherapeutic drugs lose effectiveness because of multidrug resistance developed by cancer cells. Side effects of chemotherapy and radiotherapy seriously hamper patients' quality of life. To overcome these constraints, new cancer treatment alternatives are constantly tested, including bioactive compounds of plant origin [8–10]. Polyphenol substances like e.g., coumarins [11], flavones like genistein [12], phenols like thymol [13], monotherpenes like thymoquinone [14] have been found to reduce the viability of breast cancer cell lines of various origins by mechanisms related to switching on apoptotic pathways, by blocking cell proliferation or different kinase pathways. The development of analytics with high resolution complementary instruments allows identification and determination of the molecular structure of many new active compounds from various plant species. In this respect, the complementary data obtained by Nuclear Magnetic Resonance (NMR) and Mass Spectrometry (MS) could provide reliable information for compound discovery in natural products research [15,16]. In addition, identification of bioactive compounds from various plant species is a good perspective for drug discovery, with the valuable contribution of Artificial Intelligence (AI) and synthetic chemistry, for therapy or even prevention of cancer. In the search for new therapeutic agents, there has been recent attention on the resurrection plant species. They are a group of higher plants that are able to withstand a drastic decrease in the water content of their vegetative tissues and after long periods of dryness, they are able to recover fast and fully when water is available again [17]. These plant species belong to various botanical families and live under differing environments but share high desiccation tolerance as a common characteristic. This feature makes resurrection plants a suitable model for intensive studies for stress tolerance at molecular, physiological, biochemical and metabolomics levels. The antioxidative component of resurrection plants' desiccation tolerance is well recognized [18]. Additional attention is paid to the specific secondary metabolites, constitutive or accumulated during stress, with potential application as food additives, cosmetic agents or medicinal components.

The Balkan endemite *Haberlea rhodopensis* is among the only few resurrection plants growing in Europe and as all other species on the continent, belongs to the Gesneriaceae botanical family [19]. It is among the most studied desiccation tolerant model systems, at whole plant level or as detached leaves assays [20–25].

In addition, following long established strategy [26], knowledge on the specific metabolome of *H. rhodopensis* was gradually generated and the potential application of extracts or isolated compounds in various areas has been studied, including human diseases [27–31].

The present study is the first attempt to follow the behavior of two breast cancer cell lines with different characteristics in comparison to a normal breast epithelial cell line after treatment with *H. rhodopenis* extracts and their fractions. The latter are resulting from a non-targeted approach to purify and identify highly abundant compounds involved in the significant reduction in cell viability and proliferation of the cancer cell lines. Molecular docking analysis has been performed on one of the identified compounds—myconoside to

propose a model for its interaction with several cancer proteins in an attempt to explain the potential mechanisms of its penetration in cells and the reduction in their viability and proliferation. The results are discussed as a background for further studies and potential applications.

2. Materials and Methods

2.1. Chemicals and Reagents

Acetonitril and methanol of HPLC grade from Macron Fine Chemicals™ (Avantor, Gliwice, Poland) and Acetonitril of LC/MS grade from Sigma-Aldrich (St. Louis, MO, USA) were used. Dimethyl sulfoxide (DMSO) and formic acid were sourced in analytical grade from Sigma-Aldrich (St. Louis, MO, USA). Sephadex LH-20 was purchased from Cytiva (Marlborough, MA, USA). Antibiotic/antimycotic solution was purchased from GE Healthcare (Boston, MA, USA). CD3OD was purchased from Euriso-top (Saint-Aubin, France). All reagents for cell cultures treatments and cell culture assay tests were purchased from the Sigma-Aldrich (St. Louis, MO, USA).

2.2. Plant Material and Leaf Extract Preparation and Fractionation by Size Exclusion Chromatography

H. rhodopensis plants were propagated in vitro and adapted in pots under controlled greenhouse conditions at 22–24 °C, a 16-h photoperiod, 60% relative humidity and a photon flux density of 36 μmolm^{-2} s^{-1} [32]. Fully developed leaves from well-hydrated pot plants were detached and air-dried for methanol extract preparation. Homogenised leaves (6 g) were macerated in 60 mL methanol and extracted for 30 min at 70 °C on water bath. After centrifugation at 10,000× *g* for 10 min, the supernatants were collected, dried at 40 °C by SpeedVac Labconco (Kansas City, MI, USA) and stored at −20 °C for further use.

1.1276 g of crude extract were dissolved in 14 mL methanol and subjected to size exclusion chromatography (SEC) on a Cytiva XK 50/100 column filled with Sephadex LH-20 with the help of an AKTA Pure FPLC system (Cytiva) using a constant flow of 3 mL/min of methanol. Monitoring of the elution was carried out at 220 nm. SEC fractions were collected in 50 mL tubes based on the observed elution of UV absorbing compounds.

2.3. Cell Cultures Treatments and Cell Culture Assay Tests

2.3.1. Cell Lines

In this study adherent breast cancer cell line MCF7 (ATCC cell culture collection N NTB-22TM) Manassas, Virginia, USA and MDA-MB231 (ATCC cell culture collection N HTB-26™) and normal adherent breast epithelial cell line MCF 10A (ATCC cell culture collection N CRL-10317™) Manassas, Virginia, USA) were used. The normal cell line was grown on DMEM/F12 medium and MDA-MB231 cancer cell line was grown on DMEM medium with high glucose (4.5 g/L) supplemented with 5% FBS and 10% FBS, respectively, and antibiotic/antimycotic solution Amino acid mix solution was added to the cancer cell line MDA-MB231 medium. The normal cell line needed insulin in concentration 10 μg/mL, endothelial growth factor in concentration 20 ng/mL and hydrocortisone in concentration 500 ng/mL. The cancer cell line MCF7 was incubated in DMEM with low glucose (1 g/L) supplemented with 10% FBS and antibiotic/antimycotic solution and insulin in concentration 0.01 mg/mL. Cells were incubated in 5% CO_2 incubator at 37 °C. The cells were cultivated to 80–90% confluence and were trypsinized with trypsin/EDTA solution. The cells were centrifuged, suspended in in FBS with 5–10% DMSO and stored in freezer at −150 °C.

2.3.2. MTT Cell Viability Assay

The studied cell lines were grown in 25 cm^2 well plates to confluence 80–85%. 10^4 cells were seeded per 96 well plate. The cells were grown 24 h and then treated with *H. rhodopensis* total extract (fractions). The viability was determined 48 h after the treatment with total extract and fractions at 48th, 72nd hour. MTT test followed standard procedure [33]—20 μL

of MTT stock solution (5 mg/mL) were added to the well and the cells were incubated in CO_2 incubator for 4 h. The formazan crystals were solubilized in 150 µL dimethyl sulphoxide. The color intensity was measured at wave length 600 nm (ELISA Reader Fluostar Optima/BMG Tech) ThermoFisher Scientific Corporation, Waltham, MA, USA. The untreated samples were used as control with 100% viability. The percent of viable cells in experimental conditions were scored as a percent of control sample.

$$\% \text{ of viable cells} = \text{E treated sample/E control sample} \times 100)$$

Each condition in experiment was performed in triplicate. Three biological experiments were made for each of the cell lines. The standard error bars in percent are presented in the graphs. The total extract was applied in concentrations 10, 100, 200 and 300 µg/mL, respectively, and the fractions were applied in concentration 300 µg/mL.

2.3.3. Proliferation Assay

The trypan blue-excluding proliferation assay test was made following the next procedure [33]. The cells were grown in 24-well plate to 4.5×10^4 cell for MCF10-A cell line, to 6×10^4 cells for MCF7 cell line and to 4×10^4 cells for MDA-MB231 cell line. For treatment, the medium was changed with fresh medium containing *H. rhodopensis* fractions numbers 14 and 18 at concentration 300 µg/mL. Total number of cells was counted for 96 h at 24 h interval. The cells were washed with PBS and then they were suspended in PBS, 10–20 µL of their suspension was trypan blue stained. Three biological replicates were made. The living cells presented in the graphs are averages of total number of cells in well minus averages of number of dead cells in well, stained by trypan blue dye.

2.3.4. Statistical Methods

The results are presented with standard error bars [34]. The absolute values of MTT assay of breast cancer cell lines data for total extract treatment concentration 300 µg/ml and fractions with effect on cancer cell lines are processed in ANOVA for multiple comparison plot and the data are presented extrapolated in absolute values to log2 scale. For each of the groups was applied one-way ANOVA analysis of fractions treatment versus control at each time point of the studied normal and two cancer cell lines in proliferation assay to estimate variations within the group [35].

2.4. Compound Identification

2.4.1. Semi-Preparative HPLC

Semipreparative LC analysis of SEC fractions FR14 and FR18 was performed on an Agilent 1260 Infinity II LC System (Santa Clara, CA, USA) equipped with a quaternary pump, multicolumn thermostat, autosampler and multiple wavelength detector. Separations were performed on an Agilent ZORBAX StableBond C18 (5 µm, 9.4 × 150 mm) at room temperature. SEC fraction FR14 was dissolved in 3 mL 30% methanol to a final concentration of 42 mg/mL. SEC fraction FR18 was dissolved in 3 mL 30% methanol to a final concentration of 15 mg/mL. The mobile phase consisted of water (A) and Acetonitrile (B). The flow rate was 4 mL/min. Signal was detected at 220 nm. Increasing amount of SEC fractions were injected starting from 40 µL, 60 µL, 80 µL, 100 µL, 120 µL, 140 µL and 160 µL for FR14 and 24 µL, 48 µL, 100 µL and 250 µL for FR 18 until all the amount was injected. Individual compounds were manually collected in 50 mL tubes, evaporated to dryness using Labconco CentiVap vacuum concentrator (Kansas city, USA) and used for ^{1}H NMR and LC-MS/MS analysis.

2.4.2. ^{1}H NMR

Dried semi-preparative HPLC fractions were dissolved in 600 µL of CD3OD with deuterated 25 mM 196 potassium phosphate buffer at pH 5.91 in ratio 1:1 (*v*/*v*). Proton NMR spectra were acquired on a Bruker NEO 600 spectrometer (600.18 MHz, Biospin

GmbH, Rheinstetten, Germany) at 293.0 ± 0.1 K using a Prodigy probehead. Standard parameters have been used—pulse programs zg30 and noesypr1d for experiments with water presaturation, pulse width 30°/90°, spectral width 13.66 ppm, 64 K data points, 1/64 scans, acquisition time 4.0 s, and relaxation delay 4.0 s. The signal of the rest proton signal of the solvent CD3OD at 3.3 ppm was used as an internal reference.

2.4.3. LC-MS/MS

After acquisition of ^{1}H NMR spectra, LC-MS/MS analyses was performed on an Agilent 1260 Infinity II LC System equipped with a quaternary pump, autosampler, multicolumn thermostat and Agilent 6546 QTOF detector. Analytical separations were performed on an Agilent InfinityLab Poroshell 120 SB-C18 (2.7 µm, 3 × 150 mm) (Santa Clara, CA, USA) at room temperature. ESI-MS spectra were recorded in negative ion mode between m/z 20–3200. The fragmentor energy of ESI was set to 120 V. The injection volume was 10 µL (1 mg/mL dry weight). The mobile phase consisted of 0.1% aqueous formic acid (A) and 0.1% formic acid in Acetonitrile (B). The flow rate was 0.6 mL/min. The following gradient profile was used for qualitative analysis of SEC fraction FR14: 0 min 15% B, gradient 0–20 min 18% B, 20–22 min 100% B, 22–30 min 100% B isocratic, 30–32 min to 15% B. The following gradient profile was used for qualitative analysis of SEC fraction FR18: 0 min 25% B, 0–6 min isocratic 25% B, gradient 6–12 min 42% B, 12–14 100% B, 14–24 min 100% B isocratic, 24–26 min to 25% B. Three different collision-induced dissociation (CID) energies including 10, 20 and 40 eV were used for MS/MS verification of the myconoside structure. Hyspiduline hispidulin 8-C-(6-O-acetyl-2″-O-syringoyl-β-glucopyranoside) was identified using a CID energy of 10 eV during MS/MS analysis.

2.5. Molecular Docking

For the molecular modeling we used MOL structure file of myconoside (J796.651B, Japan Chemical Substance Dictionary (Nikkaji)) as ligand and three receptor macromolecules: human glucose transporter pdb ID 4PYP [36], MYST acetyltransferase pdb ID 6OIO [37] and Estrogen Receptor pdb ID 3OS8 [38]. Complex X-ray structures, including a receptor protein bound to a low-molecular-weight ligand, were used to determine the macromolecular complexes. Prior to docking, the primary ligands were removed. 3D macromolecular docking was performed with the Seamdock [39]. For human glucose transporter Charmm-Gui membrane builder [40] has been used to orientate the transmembrane spans through lipid bilayer and the resulting supramolecular structure was used to bind to the myconoside. All structures were optimized by free energy minimum and visualized with molecular dynamics programs Chimera 1.15 [41] and protein modeling—RasTop.

3. Results

3.1. Cell Viability and Cell Proliferation

3.1.1. Cell Viability after Treatment with *Haberlea rhodopensis* Extracts and Fractions

Our preliminary experiments showed that the application of total extracts to control and breast cancer cell lines for 24 h were not informative enough. Longer exposure (for 48 h) of the cell lines to concentrations of extracts up to 300 µg/mL brought no differences in reaction to the treatment (Table S1). This triggered the application of non-target fractionation of the extracts with liquid chromatography. We obtained 21 fractions and based on the availability of a sufficient amount of dry substance, 11 were selected for further analyses, and performed with 300 µg/mL for 48 h (Table S1). The results obtained were subjected to an ANOVA (Figure 1). A significant reduction in cancer cells viability was achieved after treatment with several of the fractions, among which 14 and 18 were most effective.

To further evaluate the effect of the selected fractions 14 and 18, the treatments have been prolonged for 72 h (Figure 2). The viability of the MCF-10A normal cell line was only slightly reduced to about 80% for both fractions. The viability of MCF7 cell line was significantly reduced below 50% for both fractions, while MDA-MB231 cell line was slightly

less affected to 55% ± 10 after a treatment with fraction 14 and to 68% ± 2.2 for fraction 18 (Figure 2). The results obtained gave a good background for further proliferation assays with both fractions.

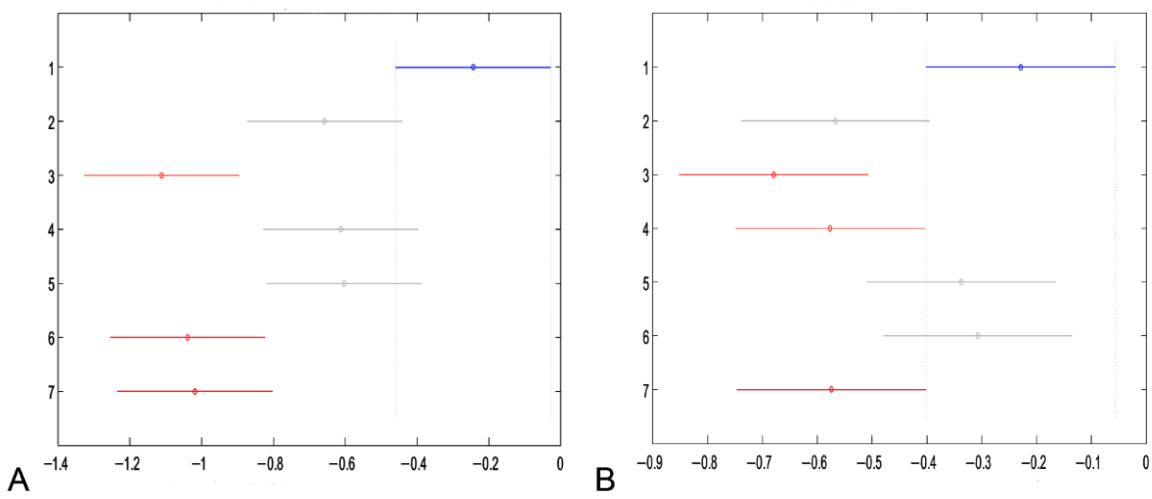

Figure 1. ANOVA multiple comparison plots of two breast cancer cell lines for statistical significance of difference between control conditions and treatment with total extract and different fractions for 48 h. (**A**) MCF7 and (**B**) MDA-MB231. Bars represent the viability of cells shown on x axis as log2 values of measured extinction for each treatment (shown on y axis); 1untreated; 2—total extract; 3—fr 14; 4—fr 15; 5—fr 16; 6—fr 17; 7—fr 18. The group tested for significance is represented with blue, with red are assigned groups with significant difference from the tested group, and with grey are shown the groups without significant changes.

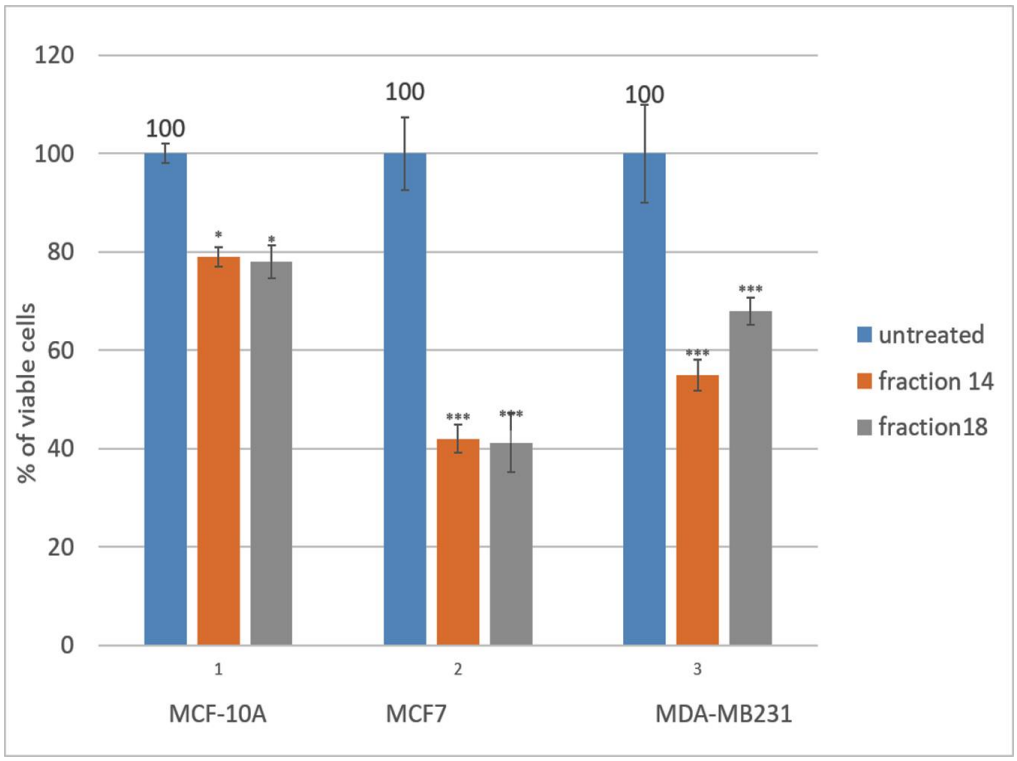

Figure 2. Cell viability of normal breast cell line MCF-10A and breast cancer cell lines MCF7 and MDA-MB231 after treatment with fractions 14 and 18 in concentration 300 µg/mL for 72 h. Untreated samples are used as controls. The standard error bars are shown in percent. *—the means are statistically significant at $p \leq 0.05$; ***—the means are statistically significant at $p \leq 0.001$.

3.1.2. Cell Proliferation Assay after Treatment with Two Selected Fractions

The proliferation assay was performed with the studied cell lines—normal MCF-10A and two cancer cell lines MCF7 and MDA-MB231 (Figure 3). The cells were treated with two *H. rhodopensis* fractions—No. 14 and 18 with a concentration of 300 µg/mL dry substance. The viable cells were scored in absolute numbers at different time points (from 24 to 96 h). The cell line MCF-10A (panel A) had a normal growth and the treated cells showed slightly reduced numbers—reaching about 82.5% of the untreated cells for fraction 14 and 75% for fraction 18 at the end of the assay. The proliferation curves of control and treated cells of line MCF7 were very different (panel B). The numbers of treated cells were reduced at each time point. This was particularly true at the end of the assay where the absolute numbers of proliferation were reduced to 37.2% (fraction 14) and 36.3% (fraction 18). The cell proliferation of triple negative cell line MDA-MB231 was also significantly reduced after treatment with the fractions (Panel C). The reduction started after 24 h treatment and continued till the end of the assay. On the other hand, the proliferation rate of the cells at the last stages of treatment—72 and 96 h formed a plateau. Nevertheless, at the end of the assay, the reduction was 40–45% in comparison with control untreated cells. It should be underlined that in both cancer lines the reduction in proliferation rate showed no differences between both fractions after 48 h of treatment. The proliferation of MCF7 cell line was slightly more reduced than that of the MDA-MB231.

3.2. Identification of Phytoactive Compounds in Plant Extract

To identify the most abundant compounds from the fractions with the strongest effects on cancer lines—Fr 14 and Fr 18 (Figure 4A), we used semi-preparative HPLC to collect the most abundant peaks for each fraction followed by ^{1}H NMR and mass spectrometry for identification (Figures 4B and 5). According to results from MS, the abundances of compounds **1** and **2** represent 24% and 14% from TIC of fractions 18 and 14, respectively (Tables S2 and S3, Figure 4A).

Semi-preparative fraction of the most abundant compound (**2**) from fraction 14 consists exclusively of myconoside as indicated by the NMR spectra (Table S4, Figure 5A). The MS and MS/MS spectra confirmed the mass of the pseudomolecular ion of myconoside (743.2399 (M – H)) as well as the presence of characteristic products of its fragmentation (Figures 4B and S1). This compound consists 14% from the total metabolite content in Fr14 followed by another unidentified compound with 6% of TIC. All other detected compounds showed very low abundances in fraction (Table S2, Figure 4A). The yield of the purified myconoside by semi-preparative fractionation was 34 mg (Figure 5A). Fr 18 shows several compounds above 6% of TIC including myconoside with 8.5% of TIC (Table S3, Figure 4B). The NMR spectra of semi-preparative fraction corresponding to the most abundant peak (23.5% of TIC) showed two main components in ratio 1.7:1, the higher concentrated one corresponding to hispidulin 8-C-(6-O-acetyl-2-O-syringoyl-β-glucopyranoside) (Table S3, Figure 5B). All signal assignments are in line with published data [42,43]. This identification was further confirmed by the corresponding pseudomolecular ion (683.1635 (M – H)) and fragmentation products from the MS^2 spectra corresponding to the loss of syringoyl and sugar moiety (Figures 5B and S2). However, further purification steps and analyses are needed for better evaluation of the active compound in this fraction.

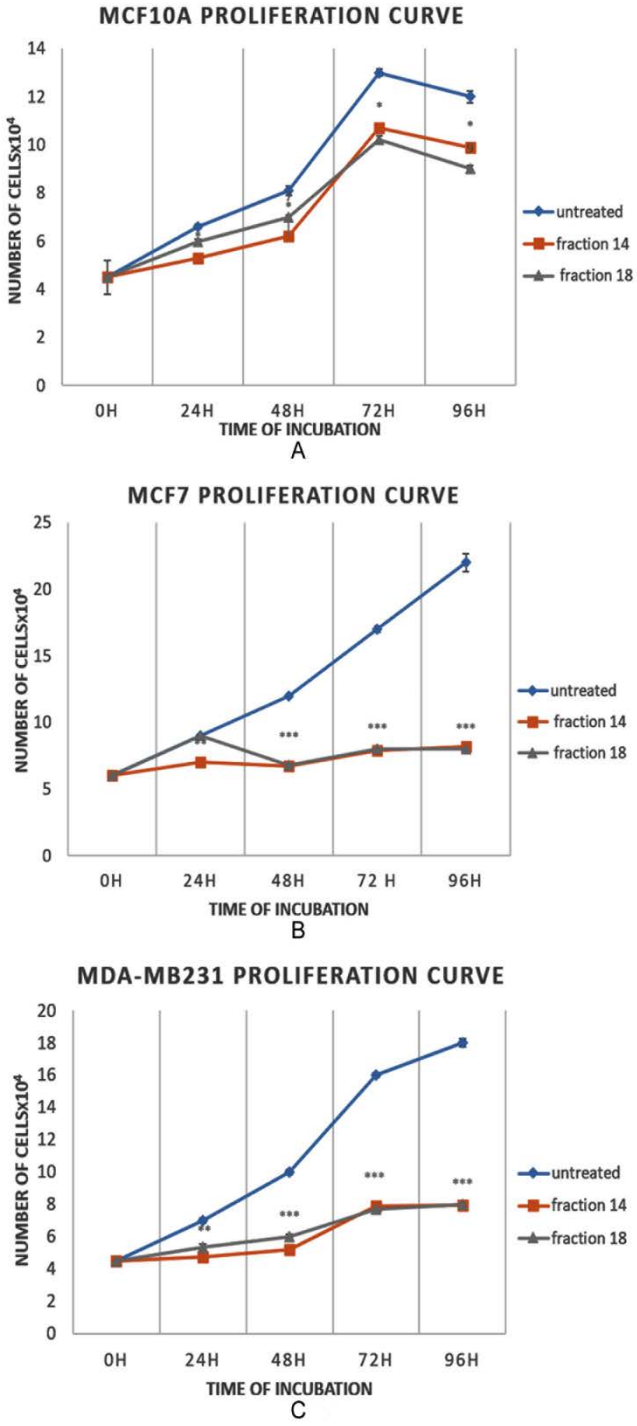

Figure 3. Proliferation curves of normal epithelial breast cell line (**A**) and breast cancer cell lines MCF7 (**B**) and MDA-MB231 (**C**) treated with *H. rhodopensis* fractions N14 and N18. The standard error bars are shown. All means at each time point are statistically significant at $p \leq 0.05$ (*), $p \leq 0.01$ (**), and $p < 0.001$ (***).

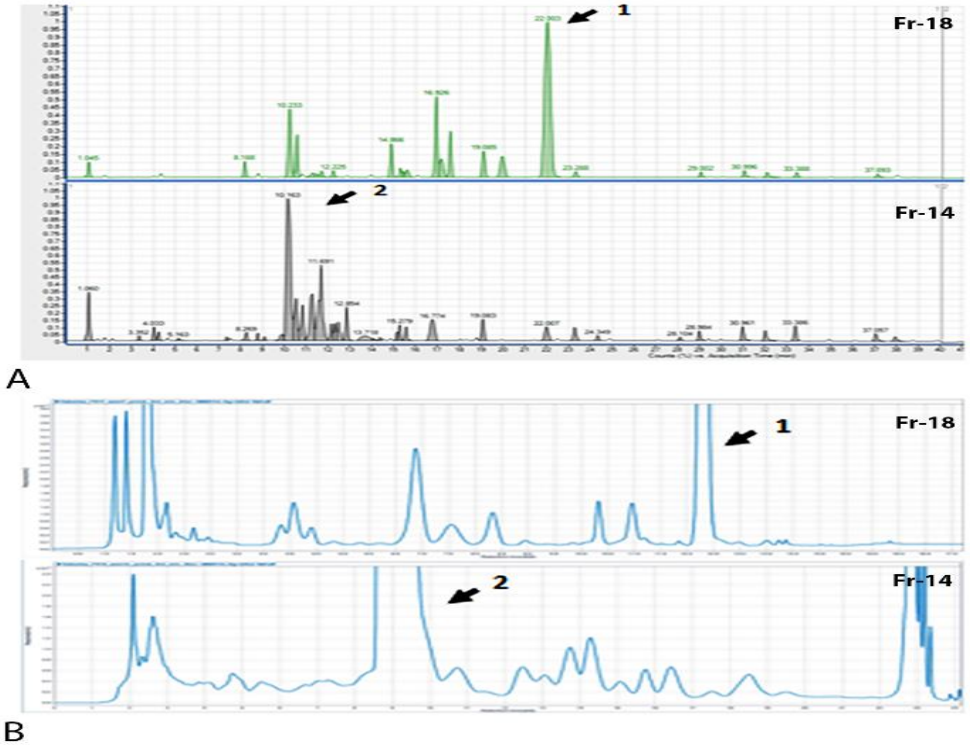

Figure 4. Mass spectrometry analysis of SEC fractions with significant effect on cancer lines and semi preparative fractionation of most abundant compounds. (**A**) Chromatograms of MS spectra of fractions 14 and 18. The most abundant peaks in each fraction are designated with numbers. (**B**) HPLC chromatograms of semi-preparative purification of the most abundant compounds from fraction 14 and 18.

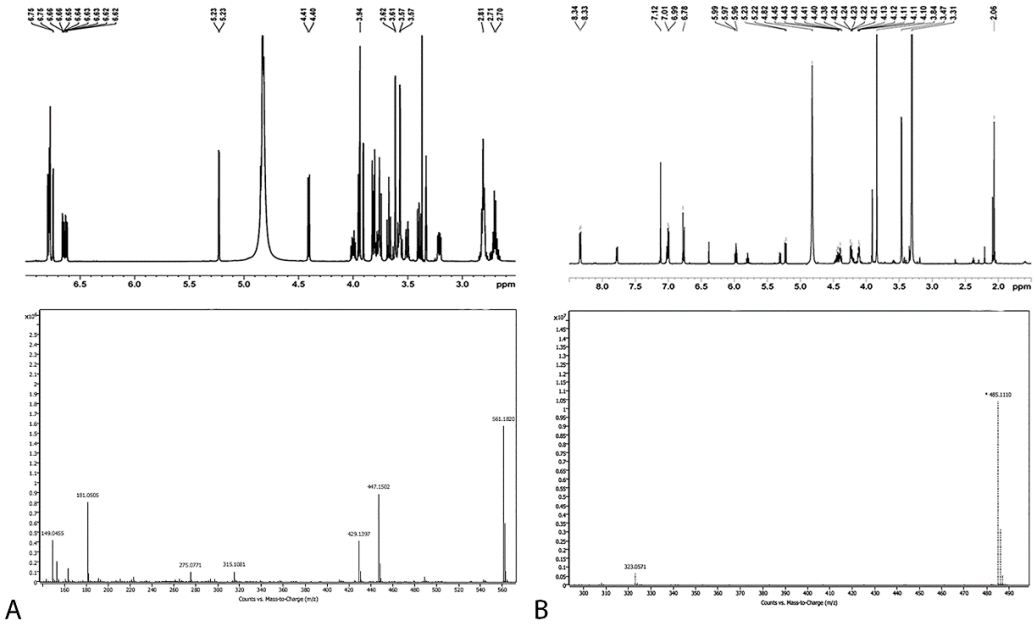

Figure 5. Identification of the most abundant compounds in fractions 14 and 18 by combined NMR/MS2 analysis on same sample. The 1H NMR spectra for each compound is represented according to chemical shift (ppm) (upper panel), while ions of fragmentation from MS2 are represented according to their m/z (lower panel). (**A**) Identification of purified myconoside (compound 2) from fraction 14. (**B**) Identification of purified hispidulin 8-C-(6-O-acetyl-2-O-syringoyl-b-glucopyranoside) from fraction 18.

3.3. Docking Analysis of Myconoside with Breast Cancer Proteins

Considering our ability to purify and identify myconoside as the main compound in Fr 14 which significantly reduced cancer cell viability and proliferation and the available 2D and 3D deposited structures, we performed flexible docking analysis of this glycoside with several breast cancer proteins involved in cellular transport, signaling and DNA modification (Figure 6A).

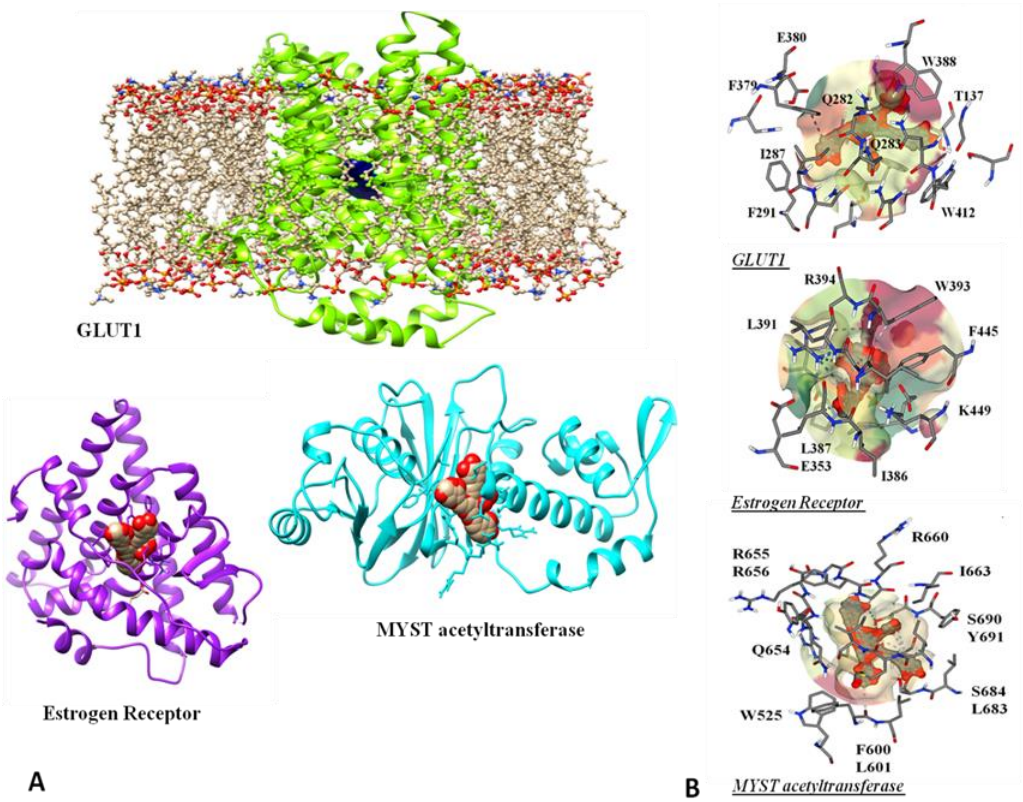

Figure 6. Molecular docking of myconoside with several protein targets from breast cancer lines. (**A**) Ribbons of three-dimensional structure of binding of myconoside with GLUT 1, MYST acetyltransferase and estrogen receptor. The protein backbone is represented as a cartoon with different colors for each protein. The docked myconoside is represented with 3D stick model of chemical formula. GLUT 1 transporter (green) is integrated and oriented in membrane phospholipid bilayer; myconoside is given in blue. (**B**) Docking of myconoside into the binding cavity of the proteins with the corresponding intermolecular interactions and amino acid residues.

Our results showed that myconoside can interact with the three tested proteins. However, the interaction with GLUT 1 displayed more binding affinity according to ΔG (−19.8 kcal/mol) than other two proteins—MYST acetyltransferase (−12.3 kcal/mol) and Estrogen Receptor (−4.2 kcal/mol). Residues of the amino acids E380, F379, F287, F291, W412, T137 and W388 from GLUT 1 transporter are involved in interactions with myconoside. The amino acid residues E353, I386, L387, L391, W393, R394, F445 and K449 of estrogen receptor are involved in the represented receptor-ligand complex; while R655, R656, R660, F663, S690, Y691, S684, L683, F600, L601, W525 and Q654 were assigned in binding pocket of MYST acetyltransferase (Figure 6B). The docking model of myconoside with GLUT 1 is mainly determined by hydrogen bonds and hydrophobic interactions of Phenylalanine and Tryptophan residues. Most interactions with estrogen receptor are in a hydrophobic manner namely by Phenylalanine and Tryptophan residues as well by Leucine and Isoleucine residues. The binding of myconoside with MYST acetyltransferase is due to hydrophobic interactions of Leucine and Isoleucine residues as well as hydrogen bonds with Arginine and Serine.

4. Discussion

Breast cancer is among the most challenging human diseases. Despite the significant progress achieved in cancer treatment, the search for new natural products continues to be very intensive. Plant metabolites are tested for possible anticancer effects. Some of them can be used as food additives for cancer prevention or as therapeutics of side effects relief after radiotherapy. Others are used to enhance the effect of conventional drugs [11,12,44,45]. In this respect, promising results were reported for the proliferation rate reduction and cytostatic effects of some plant-derived alkaloids [10,33,46]; however, their application was limited by the multi-drug resistance developed by the cancer cells. The additional burden of the side effects of chemo- or radio-therapy paves the way for further studies on new potential sources of useful compounds.

Resurrection plants are a rich source of secondary metabolites with high antioxidant potential. Here, we describe, we believe for the first time, promising results of breast cancer cell lines treatment with extracts and fractions derived from leaves of the Balkan resurrection plant species *Haberlea rhodopensis*. The application of total leaf extracts, obtained with various extraction agents led to encouraging results in studies with several human diseases, including some types of cancer [27–30]. Viability reduction was described in two prostate cancer cell lines after methanol extracts treatment [27]. The same types of extracts were reported to have unique synergetic inhibitory effects against the herpes virus [29]. In addition, they could be a good candidate to be involved in complex treatments of pathological dermatological conditions [28]. Recently [30] extensive study with six human cancer cell lines—A549 (non-small cell lung adenocarcinoma, HepG2 (hepatocellular carcinoma)), HT29 and Caco-2 (colorectal adenocarcinomas), and PC3 and DU145 (prostate adenocarcinomas) showed that alcohol extraction appeared to be more effective than the aqueous. Significant antimigratory concentration-dependent effects were achieved for non-small cell lung adenocarcinoma and hepatocellular carcinoma (HepG2) cell lines [30].

Our study showed that the total extract was unable to significantly reduce the viability of the MCF7 and MDA-MB231 breast cancer cell lines (Supplementary Table S1). This triggered our further efforts to fractionate the extracts to achieve enrichment of active substances. Two of the fractions (14 and 18) showed significant effects on breast cancer cell viability (Figure 1) and a negligible effect on normal breast epithelia cell line MCF10-A (Supplementary Table S1, Figure 2). These fractions had a high impact on cell proliferation of the studied breast cancer cell lines and an insignificant effect on the proliferation of the normal breast epithelial cell line. One of the fractions (Fr 14) is enriched of myconoside and another one (Fr 18)—of hispidulin 8-C-(6-O-acetyl-2″-O-syringoyl-β-glu-copyranoside) (Figure 4).

4.1. Potential Role of Myconoside

Myconoside has been isolated earlier from the three European members of Gesnereiacea, including *H. rhodopensis* [42,47–51]. The myconoside molecule has a phenyl glycoside structure with 12 hydroxyl groups (Supplementary Figure S1) which determined its chemical activity and possibility to form a 3D structure which was deposited in the Japan Chemical Substance Dictionary (Nikkaji) database. The structure file was used to propose models of its binding to three proteins with an essential role for breast cancer and breast cancer cell lines development—estrogen receptor, glucose transporter GLUT1 and MYST acetyltrasferase (Figure 6). All of these three proteins are expressed in the MCF7 cell line whereas two of them—GLUT1 and MYST acetyltrasferase are expressed in MB-MDA231. We presumed a possibility for myconoside binding to glucose transporter GLUT1. The GLUT family of transporters are localized on the cell membrane and are connected by hydrophilic loops [52]. They are expressed in high levels in different types of tumors, including breast tumors [53–55] and in particular in the two cancer cell lines under study—MCF7 and MDA-MB231 [6]. The chemically synthesized transporter inhibitors WZB117 and STF-31 block cell proliferation of MCF7 and MDA-MB231 cell lines by an increase in extracellular glucose and a decrease in extracellular lactose [55]. WZB27 and

WZB115 are two transporter inhibitors which reduce glucose uptake and block cell proliferation in MCF7 cell line [56]. Various polyphenol substances of plant origin—gossypol, genistein, resveratrol, quercetin have been described to influence glucose metabolism in breast cancer cell lines [7]. We have two hypotheses about myconoside binding to the glucose transporter. It could be a glucose transporter blocker, thus reducing glucose uptake in cells, or this could be the way for myconoside penetration in the cell. The prediction of molecular binding of myconoside with GLUT1 transporter makes possible the penetration of myconoside in cancer cells by binding to this membrane localized transporter. These hypotheses should be a subject of future studies.

The estrogen receptor has an essential role for estrogen-dependent growth in estrogen expressing tumors and cancer cell lines. We presume a possible binding of myconoside to the estrogen receptor of the MCF7 cell line—a good model to search possibilities for estrogen receptor agonists/antagonists in breast cancer therapy [57]. Drugs with polyphenyl structures block the DNA binding receptor domain and are competitive antagonists of estradiol. This is a mechanism for hormone dependent growth blockage of breast cancer cells [57,58]. Such estrogen antagonists of plant origin are the coumarins with antiproliferative effects on the breast cancer cell line MDA-MB435 [57]. We propose a role of myconoside as an estrogen receptor modulator. Plant substances were virtually screened and 162 of them have been validated by docking with estrogen receptor α. Eight of them have ER α competition effects. Genistein, daidzein, phloretin, ellagic acid, ursolic acid, (−)-epigallocatechin-3-gallate, kaempferol are with different antagonistic activities against estrogen receptor α [59].

Our docking analyses allowed the presumption that another target of myconoside could be MYST acetyltransferase. This could be a mechanism, affecting cell proliferation in studied breast cell lines related to epigenetic DNA regulation. We found that interactions of MYST acetyltransferase with myconoside are docked by amino acids residues ARG655, LEU686, GLN760, ARG660, LEU689 and LYS763, which are previously reported to interact with different compounds of the medicinal plant *Withania somnifera* (L.) [60]. The MYST acetiytransferases are related to the activation of estrogen receptor α by acetylation of the hystone acetyltransferase domain in the estrogen receptor promotor. This mechanism of epigenetic regulation activates the estrogen receptor expression in estrogen receptor positive breast cancer cell lines like MCF7 [7]. The blockage of acetyltransferase enzyme suppresses the activation of estrogen receptor α promotor. Studies of acetyltransferase mRNA and protein expression showed different levels of their expression in a panel of breast cancer cell lines [7]. This is a pathway to limit estrogen dependent growth in estrogen receptor positive cells and could be a possible explanation for the higher inhibitory effect on the triple positive cell line MCF7. Purified myconoside was shown to have antimygratory effects and cell proliferation blockage on the A549 lung adenocarcinoma cell line with an IC50 of 20 μg/mL [61]. Our results showed that fractions containing myconoside did not significantly affect cell viability or proliferation of the normal cell line MCF10A (Figures 2 and 3). This is in agreement with the report that *H. rhodopensis* extracts fractions with identified myconoside and calceolarioside E has effects on protein expression of neutrophil essential transcription factor regulating redox potential Nrf2 in bone marrow neutrophils [42]. In addition, when applied in low concentrations, the natural phenyl glycoside induces hormetic-like response in MDCKII cell line [62] or has photoprotective effects on UVA/UVB irradiated immortalized keratinocytes [53].

4.2. Potential Role of Hispidulin 8-C-(6-O-acetyl-2″-O-syringoyl-β-glu-copyranoside)

The proliferation rate was significantly reduced in both breast cancer cell lines after treatment with Fraction 18. This fraction is more complex, containing several compounds, including myconoside and hispidulin 8-C-(6-O-acetyl-2″-O-syringoyl-β-glu-copyranoside). We identified the most abundant compound as hispidulin 8-C-(6-O-acetyl-2″-O-syringoyl-β-glu-copyranoside) (Figure 5B). It was reported earlier in a mixture of flavone glycosides of the same plant species [43,63]. While myconoside is found exceptionally in some

Gesmneriaceae resurrection plant species, hispidulin is common for many plant species widely applicable in traditional medicine, such as *Grindelia argentina*, *Arrabidaea chica*, *Saussurea involucrate*, *Crossostephium chinense*, *Artemisia* and *Salvia* species. It was shown to possess various activities—antioxidant, antifungal, anti-inflammatory, antimutagenic, and antitumor [64]. The potential therapeutic usefulness of hispidulin has been studied in a variety of tumors [65–68]. The molecular mechanisms mediating its effects on cancer cell lines of different origin have been analyzed. Effects on cell viability and proliferation have been established for prostate cancer cell lines [65], GLUT1-HEK293T transformed cells and Hep2G hepatocellular carcinoma cells [66], as well as for human melanoma A253 cancer cells [67]. Its mechanism of influence on cell signal pathways depends on the type of cancer. In the case of prostate cancer cell lines it is related to limitation of cell migration, invasion, proliferation and apoptosis initiation mediated via PPARγ activation and autophagy induction [65]. Hispidulin modulates epithelial-mesenchymal transition in breast cancer cells—a process associated with the disruption of cell junctions, increase in cell mobility and metastasis by suppressing the TGF-β1-induced Smad2/3 signaling pathway [68]. The effects on human melanoma cells are mediated by activation of apoptosis rather than autophagy, inhibiting kinase signaling pathways AKT and ERK [4]. Recently, the inhibitory effect of various flavonoids on GLUT1 transporter in HEK293T and HepG2 has been reported [66]. Several flavonoids, including hispidulin inhibit hepatocellular carcinoma cell line Hep2G and GLUT1 expressing HEK2893T cell line by binding to glucose transporter1, which was shown by docking analysis and validated [66]. The suppression of GLUT1 transporter activity by hispidulin was established to 40% of control untreated sample at the concentration range 100–150 μM. This fact could explain our results on cell viability reduction and suppression of proliferation in the studied cell line MCF7 and MDA-MB231, which both express GLUT1 in high levels and are characterized with intensive glucose metabolism. The combination of identified hispidulin 8-C-(6-O-acetyl-2″-O-syringoyl-β-glu- copyranoside) and the second highly abundant unidentified substance in the fraction should be a subject of future investigations related to its identification and the clarification of molecular mechanisms of influence on breast cancer cell proliferation.

5. Conclusions

This study described for the first time the effect of *H. rhodopensis* methanol extract fractions on the viability and proliferation of two breast cancer cell lines with different characteristics and a normal cell line. The inhibitory effects are specific for cancer cell lines and are better for the hormone responsive one. Myconoside appears to be a suitable agent for cancer therapy and a possible model for its action was proposed, targeting three specific cancer hallmark proteins.

Supplementary Materials: The following supporting information can be downloaded at: https://www.mdpi.com/article/10.3390/separations10070388/s1. Table S1. cell viability, Table S2. Metabolic content of fraction 14, Table S3. Metabolic content of fraction 18, Table S4. signals of ^{1}H and ^{13}C of myconoside, Table S5. ^{1}H signals of hispidulin, Figure S1. Molecular structure of myconoside (MS/MS identification), Figure S2. Molecular structure of hispidulin (MS/MS identification), Figure S3. Structure of myconoside (NMR), Figure S4. Structure of hispidulin (NMR).

Author Contributions: Conceptualization, D.Z. and P.M.; methodology, D.Z. and P.M.; validation, D.Z., P.M., K.R. and S.S.; formal analysis, D.Z., P.M., S.S. and K.R.; investigation, D.Z., P.M., S.S., K.R., S.Z., L.S.-S., D.M. and D.D.; resources, D.Z., L.S.-S., D.D., S.S. and K.R.; writing—original draft preparation, D.Z., P.M., D.M., L.S.-S. and D.D.; writing—review and editing, D.Z., P.M., S.S., K.R., S.Z., L.S.-S., D.M. and D.D.; visualization, D.Z., P.M., S.S. and K.R.; supervision, D.Z., P.M., S.S. and D.D.; project administration, D.Z., P.M., D.D. and L.S.-S.; funding acquisition, D.Z. All authors have read and agreed to the published version of the manuscript.

Funding: The research was funded by NSF of Bulgaria, Grant number КП-06-Н41/6, Operational Program Science and Education for Smart Growth 2014–2020, co-financed by the European Union through the European Structural and Investment Funds, Grant BG05M2OP001-1.002-0012.

Data Availability Statement: Data is contained within the article.

Acknowledgments: The authors highly appreciate the help of Zlatina Gospodinova (Institute of Plant Physiology and Genetics, Bulgarian Academy of Sciences) by kindly providing cell line MCF-10A and of Radostina Alexandrova (Institute of Experimental Morphology and Anthropology Bulgarian Academy of Sciences, Bulgarian Academy of Sciences) for kindly providing MCF7 cell line and of Milena Mourdjeva (Institute of Biology and Immunology of Reproduction, Bulgarian Academy of Sciences) for kindly providing cell line MDA-MB231. We highly appreciate the help of Svetlana Hristova, Ph.D (Department of Medical Physics and Biophysics, Medical Faculty, Medical University–Sofia, Zdrave Str. 2, 1431 Sofia, Bulgaria) for kindly contribute with software for analyses of molecular docking.

Conflicts of Interest: The authors declare no conflict of interest.

References

1. Lancet, T. Breast Cancer in Developing Countries. *Lancet* **2009**, *374*, 1567. [CrossRef]
2. Arnold, M.; Morgan, E.; Rumgay, H.; Mafra, A.; Singh, D.; Laversanne, M.; Vignat, J.; Gralow, J.R.; Cardoso, F.; Siesling, S.; et al. Current and Future Burden of Breast Cancer: Global Statistics for 2020 and 2040. *Breast* **2022**, *66*, 15–23. [CrossRef]
3. Breast Cancer Facts & Statistics 2023. Available online: https://www.breastcancer.org/facts-statistics (accessed on 27 March 2023).
4. Shrihastini, V.; Muthuramalingam, P.; Adarshan, S.; Sujitha, M.; Chen, J.-T.; Shin, H.; Ramesh, M. Plant Derived Bioactive Compounds, Their Anti-Cancer Effects and In Silico Approaches as an Alternative Target Treatment Strategy for Breast Cancer: An Updated Overview. *Cancers* **2021**, *13*, 6222. [CrossRef] [PubMed]
5. George, B.P.A.; Abrahamse, H. A Review on Novel Breast Cancer Therapies: Photodynamic Therapy and Plant Derived Agent Induced Cell Death Mechanisms. *Anticancer Agents Med. Chem.* **2016**, *16*, 793–801. [CrossRef]
6. Barbosa, A.M.; Martel, F. Targeting Glucose Transporters for Breast Cancer Therapy: The Effect of Natural and Synthetic Compounds. *Cancers* **2020**, *12*, 154. [CrossRef] [PubMed]
7. Yu, L.; Liang, Y.; Cao, X.; Wang, X.; Gao, H.; Lin, S.-Y.; Schiff, R.; Wang, X.-S.; Li, K. Identification of MYST3 as a Novel Epigenetic Activator of ERα Frequently Amplified in Breast Cancer. *Oncogene* **2017**, *36*, 2910–2918. [CrossRef] [PubMed]
8. Ali Abdalla, Y.O.; Subramaniam, B.; Nyamathulla, S.; Shamsuddin, N.; Arshad, N.M.; Mun, K.S.; Awang, K.; Nagoor, N.H. Natural Products for Cancer Therapy: A Review of Their Mechanism of Actions and Toxicity in the Past Decade. *J. Trop. Med.* **2022**, *2022*, e5794350. [CrossRef] [PubMed]
9. Lopes, C.M.; Dourado, A.; Oliveira, R. Phytotherapy and Nutritional Supplements on Breast Cancer. *BioMed Res. Int.* **2017**, *2017*, e7207983. [CrossRef]
10. Mazurakova, A.; Koklesova, L.; Samec, M.; Kudela, E.; Kajo, K.; Skuciova, V.; Csizmár, S.H.; Mestanova, V.; Pec, M.; Adamkov, M.; et al. Anti-Breast Cancer Effects of Phytochemicals: Primary, Secondary, and Tertiary Care. *EPMA J.* **2022**, *13*, 315–334. [CrossRef]
11. Küpeli Akkol, E.; Genç, Y.; Karpuz, B.; Sobarzo-Sánchez, E.; Capasso, R. Coumarins and Coumarin-Related Compounds in Pharmacotherapy of Cancer. *Cancers* **2020**, *12*, 1959. [CrossRef]
12. Li, Z.; Li, J.; Mo, B.; Hu, C.; Liu, H.; Qi, H.; Wang, X.; Xu, J. Genistein Induces Cell Apoptosis in MDA-MB-231 Breast Cancer Cells via the Mitogen-Activated Protein Kinase Pathway. *Toxicol. In Vitro* **2008**, *22*, 1749–1753. [CrossRef] [PubMed]
13. Melo, J.O.; Fachin, A.L.; Rizo, W.F.; Jesus, H.C.R.; Arrigoni-Blank, M.F.; Alves, P.B.; Marins, M.A.; França, S.C.; Blank, A.F. Cytotoxic Effects of Essential Oils from Three Lippia Gracilis Schauer Genotypes on HeLa, B16, and MCF-7 Cells and Normal Human Fibroblasts. *Genet. Mol. Res.* **2014**, *13*, 2691–2697. [CrossRef]
14. Woo, C.C.; Hsu, A.; Kumar, A.P.; Sethi, G.; Tan, K.H.B. Thymoquinone Inhibits Tumor Growth and Induces Apoptosis in a Breast Cancer Xenograft Mouse Model: The Role of P38 MAPK and ROS. *PLoS ONE* **2013**, *8*, e75356. [CrossRef] [PubMed]
15. Borges, R.M.; Resende, J.V.M.; Pinto, A.P.; Garrido, B.C. Exploring Correlations between MS and NMR for Compound Identification Using Essential Oils: A Pilot Study. *Phytochem. Anal.* **2022**, *33*, 533–542. [CrossRef]
16. Leggett, A.; Wang, C.; Li, D.-W.; Somogyi, A.; Bruschweiler-Li, L.; Brüschweiler, R. Identification of Unknown Metabolomics Mixture Compounds by Combining NMR, MS, and Cheminformatics. *Methods Enzymol.* **2019**, *615*, 407–422. [CrossRef] [PubMed]
17. Gaff, D.F.; Oliver, M. The Evolution of Desiccation Tolerance in Angiosperm Plants: A Rare yet Common Phenomenon. *Funct Plant Biol.* **2013**, *40*, 315–328. [CrossRef]
18. Dinakar, C.; Bartels, D. Desiccation Tolerance in Resurrection Plants: New Insights from Transcriptome, Proteome and Metabolome Analysis. *Front. Plant Sci.* **2013**, *4*, 482. [CrossRef]
19. Legardón, A.; García-Plazaola, J.I. Gesneriads, a Source of Resurrection and Double-Tolerant Species: Proposal of New Desiccation- and Freezing-Tolerant Plants and Their Physiological Adaptations. *Biology* **2023**, *12*, 107. [CrossRef]
20. Ivanova, A.; O'Leary, B.; Signorelli, S.; Falconet, D.; Moyankova, D.; Whelan, J.; Djilianov, D.; Murcha, M.W. Mitochondrial Activity and Biogenesis during Resurrection of *Haberlea rhodopensis*. *New Phytol.* **2022**, *236*, 943–957. [CrossRef]
21. Liu, J.; Moyankova, D.; Lin, C.-T.; Mladenov, P.; Sun, R.-Z.; Djilianov, D.; Deng, X. Transcriptome Reprogramming during Severe Dehydration Contributes to Physiological and Metabolic Changes in the Resurrection Plant *Haberlea rhodopensis*. *BMC Plant Biol.* **2018**, *18*, 351. [CrossRef]

22. Mladenov, P.; Zasheva, D.; Planchon, S.; Leclercq, C.C.; Falconet, D.; Moyet, L.; Brugière, S.; Moyankova, D.; Tchorbadjieva, M.; Ferro, M.; et al. Proteomics Evidence of a Systemic Response to Desiccation in the Resurrection *Plant Haberlea rhodopensis*. *Int. J. Mol. Sci.* **2022**, *23*, 8520. [CrossRef] [PubMed]
23. Vassileva, V.; Moyankova, D.; Dimitrova, A.; Mladenov, P.; Djilianov, D. Assessment of Leaf Micromorphology after Full Desiccation of Resurrection Plants. *Plant Biosyst.* **2019**, *153*, 108–117. [CrossRef]
24. Mladenov, P.; Finazzi, G.; Bligny, R.; Moyankova, D.; Zasheva, D.; Boisson, A.-M.; Brugière, S.; Krasteva, V.; Alipieva, K.; Simova, S.; et al. In Vivo Spectroscopy and NMR Metabolite Fingerprinting Approaches to Connect the Dynamics of Photosynthetic and Metabolic Phenotypes in Resurrection Plant *Haberlea rhodopensis* during Desiccation and Recovery. *Front. Plant Sci.* **2015**, *6*, 564. [CrossRef] [PubMed]
25. Kuroki, S.; Tsenkova, R.; Moyankova, D.; Muncan, J.; Morita, H.; Atanassova, S.; Djilianov, D. Water Molecular Structure Underpins Extreme Desiccation Tolerance of the Resurrection Plant *Haberlea rhodopensis*. *Sci. Rep.* **2019**, *9*, 3049. [CrossRef] [PubMed]
26. Djilianov, D.; Ivanov, S.; Georgieva, T.; Moyankova, D.; Berkov, S.; Petrova, G.; Mladenov, P.; Christov, N.; Hristozova, N.; Peshev, D.; et al. A Holistic Approach to Resurrection Plants. *Haberlea rhodopensis —A Case Study. Biotechnol. Biotechnol. Equip.* **2009**, *23*, 1414–1416. [CrossRef]
27. Hayrabedyan, S.; Todorova, K.; Zasheva, D.; Moyankova, D.; Georgieva, D.; Todorova, J.; Djilianov, D. *Haberlea rhodopensis* Has Potential as a New Drug Source Based on Its Broad Biological Modalities. *Biotechnol. Biotechnol. Equip.* **2013**, *27*, 3553–3560. [CrossRef]
28. Kostadinova, A.; Doumanov, J.; Moyankova, D.; Ivanov, S.; Mladenova, K.; Djilianov, D.; Topuzova-Hristova, T. *Haberlea rhodopensis* Extracts Affect Cell Periphery of Keratinocytes. *Comptes Rendus Acad. Bulg. Sci.* **2016**, *69*, 439–448.
29. Moyankova, D.; Hinkov, A.; Shishkov, S.; Djilianov, D. Inhibitory Effect of Extracts from *Haberlea rhodopensis* Friv. against Herpes Simplex Virus. *Comptes Rendus Acad. Bulg. Sci.* **2014**, *76*, 1369–1376.
30. Spyridopoulou, K.; Kyriakou, S.; Nomikou, A.; Roupas, A.; Ermogenous, A.; Karamanoli, K.; Moyankova, D.; Djilianov, D.; Galanis, A.; Panayiotidis, M.I.; et al. Chemical Profiling, Antiproliferative and Antimigratory Capacity of *Haberlea rhodopensis* Extracts in an In Vitro Platform of Various Human Cancer Cell Lines. *Antioxidants* **2022**, *11*, 2305. [CrossRef]
31. Djilianov, D.; Genova, G.; Parvanova, D.; Zapryanova, N.; Konstantinova, T.; Atanassov, A. In Vitro Culture of the Resurrection Plant *Haberlea rhodopensis*. *Plant Cell Tiss. Organ Cult.* **2005**, *80*, 115–118. [CrossRef]
32. Mosmann, T. Rapid Colorimetric Assay for Cellular Growth and Survival: Application to Proliferation and Cytotoxicity Assays. *J. Immunol. Methods* **1983**, *65*, 55–63. [CrossRef]
33. Soprano, M.; Sorriento, D.; Rusciano, M.R.; Maione, A.S.; Limite, G.; Forestieri, P.; D'Angelo, D.; D'Alessio, M.; Campiglia, P.; Formisano, P.; et al. Oxidative Stress Mediates the Antiproliferative Effects of Nelfinavir in Breast Cancer Cells. *PLoS ONE* **2016**, *11*, e0155970. [CrossRef]
34. Standard Error Calculator (High Precision). Available online: https://miniwebtool.com/standard-error-calculator/ (accessed on 27 March 2023).
35. One-Way ANOVA Calculator, Plus Tukey HSD. Available online: https://www.socscistatistics.com/tests/anova/default2.aspx (accessed on 27 March 2023).
36. Deng, D.; Xu, C.; Sun, P.; Wu, J.; Yan, C.; Hu, M.; Yan, N. Crystal Structure of the Human Glucose Transporter GLUT1. *Nature* **2014**, *510*, 121–125. [CrossRef] [PubMed]
37. Leaver, D.J.; Cleary, B.; Nguyen, N.; Priebbenow, D.L.; Lagiakos, H.R.; Sanchez, J.; Xue, L.; Huang, F.; Sun, Y.; Mujumdar, P.; et al. Discovery of Benzoylsulfonohydrazides as Potent Inhibitors of the Histone Acetyltransferase KAT6A. *J. Med. Chem.* **2019**, *62*, 7146–7159. [CrossRef]
38. Bruning, J.B.; Parent, A.A.; Gil, G.; Zhao, M.; Nowak, J.; Pace, M.C.; Smith, C.L.; Afonine, P.V.; Adams, P.D.; Katzenellenbogen, J.A.; et al. Coupling of Receptor Conformation and Ligand Orientation Determine Graded Activity. *Nat. Chem. Biol.* **2010**, *6*, 837–843. [CrossRef]
39. Morris, G.M.; Huey, R.; Lindstrom, W.; Sanner, M.F.; Belew, R.K.; Goodsell, D.S.; Olson, A.J. AutoDock4 and AutoDockTools4: Automated Docking with Selective Receptor Flexibility. *J. Comput. Chem.* **2009**, *30*, 2785–2791. [CrossRef] [PubMed]
40. Wu, E.L.; Cheng, X.; Jo, S.; Rui, H.; Song, K.C.; Dávila-Contreras, E.M.; Qi, Y.; Lee, J.; Monje-Galvan, V.; Venable, R.M.; et al. CHARMM-GUI Membrane Builder toward Realistic Biological Membrane Simulations. *J. Comput. Chem.* **2014**, *35*, 1997–2004. [CrossRef] [PubMed]
41. Pettersen, E.F.; Goddard, T.D.; Huang, C.C.; Couch, G.S.; Greenblatt, D.M.; Meng, E.C.; Ferrin, T.E. UCSF Chimera—A Visualization System for Exploratory Research and Analysis. *J. Comput. Chem.* **2004**, *25*, 1605–1612. [CrossRef] [PubMed]
42. Amirova, K.M.; Dimitrova, P.A.; Marchev, A.S.; Krustanova, S.V.; Simova, S.D.; Alipieva, K.I.; Georgiev, M.I. Biotechnologically-Produced Myconoside and Calceolarioside E Induce Nrf2 Expression in Neutrophils. *Int. J. Mol. Sci.* **2021**, *22*, 1759. [CrossRef]
43. Ebrahimi, S.N.; Gafner, F.; Dell'Acqua, G.; Schweikert, K.; Hamburger, M. Flavone 8-C-Glycosides from *Haberlea rhodopensis* Friv. (Gesneriaceae). *Helv. Chim. Acta* **2011**, *94*, 38–45. [CrossRef]
44. Brenton, J.D.; Carey, L.A.; Ahmed, A.A.; Caldas, C. Molecular Classification and Molecular Forecasting of Breast Cancer: Ready for Clinical Application? *J. Clin. Oncol.* **2005**, *23*, 7350–7360. [CrossRef] [PubMed]
45. Demain, A.L.; Vaishnav, P. Natural Products for Cancer Chemotherapy. *Microb. Biotechnol.* **2011**, *4*, 687–699. [CrossRef]

46. Mazumder, K.; Biswas, B.; Raja, I.M.; Fukase, K. A Review of Cytotoxic Plants of the Indian Subcontinent and a Broad-Spectrum Analysis of Their Bioactive Compounds. *Molecules* **2020**, *25*, 1904. [CrossRef] [PubMed]
47. Moyankova, D.; Mladenov, P.; Berkov, S.; Peshev, D.; Georgieva, D.; Djilianov, D. Metabolic Profiling of the Resurrection Plant *Haberlea rhodopensis* during Desiccation and Recovery. *Physiol. Plant.* **2014**, *152*, 675–687. [CrossRef]
48. Cañigueral, S.; Salvía, M.J.; Vila, R.; Iglesias, J.; Virgili, A.; Parella, T. New Polyphenol Glycosides from *Ramonda myconi*. *J. Nat. Prod.* **1996**, *59*, 419–422. [CrossRef]
49. Jensen, S.R. Caffeoyl Phenylethanoid Glycosides in *Sanango racemosum* and in the Gesneriaceae. *Phytochemistry* **1996**, *43*, 777–783. [CrossRef]
50. Kondeva-Burdina, M.; Zheleva-Dimitrova, D.; Nedialkov, P.; Girreser, U.; Mitcheva, M. Cytoprotective and Antioxidant Effects of Phenolic Compounds from *Haberlea rhodopensis* Friv. (Gesneriaceae). *Pharmacogn. Mag.* **2013**, *9*, 294–301. [CrossRef]
51. Gođevac, D.; Ivanović, S.; Simić, K.; Anđelković, B.; Jovanović, Ž.; Rakić, T. Metabolomics Study of the Desiccation and Recovery Process in the Resurrection Plants *Ramonda serbica* and *R. nathaliae*. *Phytochem. Anal.* **2022**, *33*, 961–970. [CrossRef]
52. Mueckler, M.; Thorens, B. The SLC2 (GLUT) Family of Membrane Transporters. *Mol. Asp. Med.* **2013**, *34*, 121–138. [CrossRef]
53. Szablewski, L. Expression of Glucose Transporters in Cancers. *Biochim. Biophys. Acta* **2013**, *1835*, 164–169. [CrossRef]
54. Medina, R.A.; Owen, G.I. Glucose Transporters: Expression, Regulation and Cancer. *Biol. Res.* **2002**, *35*, 9–26. [CrossRef]
55. Xintaropoulou, C.; Ward, C.; Wise, A.; Marston, H.; Turnbull, A.; Langdon, S.P. A Comparative Analysis of Inhibitors of the Glycolysis Pathway in Breast and Ovarian Cancer Cell Line Models. *Oncotarget* **2015**, *6*, 25677–25695. [CrossRef]
56. Liu, Y.; Zhang, W.; Cao, Y.; Liu, Y.; Bergmeier, S.; Chen, X. Small Compound Inhibitors of Basal Glucose Transport Inhibit Cell Proliferation and Induce Apoptosis in Cancer Cells via Glucose-Deprivation-like Mechanisms. *Cancer Lett.* **2010**, *298*, 176–185. [CrossRef] [PubMed]
57. Jameera Begam, A.; Jubie, S.; Nanjan, M.J. Estrogen Receptor Agonists/Antagonists in Breast Cancer Therapy: A Critical Review. *Bioorganic Chem.* **2017**, *71*, 257–274. [CrossRef]
58. Thomas, M.P.; Potter, B.V.L. Estrogen O-Sulfamates and Their Analogues: Clinical Steroid Sulfatase Inhibitors with Broad Potential. *J. Steroid Biochem. Mol. Biol.* **2015**, *153*, 160–169. [CrossRef]
59. Pang, X.; Fu, W.; Wang, J.; Kang, D.; Xu, L.; Zhao, Y.; Liu, A.-L.; Du, G.-H. Identification of Estrogen Receptor α Antagonists from Natural Products via In Vitro and In Silico Approaches. *Oxid. Med. Cell. Longev.* **2018**, *2018*, 6040149. [CrossRef] [PubMed]
60. Deshpande, S.H.; Muhsinah, A.B.; Bagewadi, Z.K.; Ankad, G.M.; Mahnashi, M.H.; Yaraguppi, D.A.; Shaikh, I.A.; Khan, A.A.; Hegde, H.V.; Roy, S. In Silico Study on the Interactions, Molecular Docking, Dynamics and Simulation of Potential Compounds from *Withania somnifera* (L.) Dunal Root against Cancer by Targeting KAT6A. *Molecules* **2023**, *28*, 1117. [CrossRef]
61. Kostadinova, A.; Hazarosova, R.; Topouzova-Hristova, T.; Moyankova, D.; Yordanova, V.; Veleva, R.; Nikolova, B.; Momchilova, A.; Djilianov, D.; Staneva, G. Myconoside Interacts with the Plasma Membranes and the Actin Cytoskeleton and Provokes Cytotoxicity in Human Lung Adenocarcinoma A549 Cells. *J. Bioenerg. Biomembr.* **2022**, *54*, 31–43. [CrossRef]
62. Kostadinova, A.; Staneva, G.; Topouzova-Hristova, T.; Moyankova, D.; Yordanova, V.; Veleva, R.; Nikolova, B.; Momchilova, A.; Djilianov, D.; Hazarosova, R. Myconoside Affects the Viability of Polarized Epithelial MDCKII Cell Line by Interacting with the Plasma Membrane and the Apical Junctional Complexes. *Separations* **2022**, *9*, 239. [CrossRef]
63. Zheleva-Dimitrova, D.; Nedialkov, P.; Giresser, U. A Validated HPLC Method for Simultaneous Determination of Caffeoyl Phenylethanoid Glucosides and Flavone 8-C-Glycosides in *Haberlea rhodopensis*. *Nat. Prod. Commun.* **2016**, *11*, 791–792. [CrossRef] [PubMed]
64. Patel, K.; Patel, D.K. Medicinal Importance, Pharmacological Activities, and Analytical Aspects of Hispidulin: A Concise Report. *J. Tradit. Complement. Med.* **2016**, *7*, 360–366. [CrossRef] [PubMed]
65. Wang, Y.; Guo, S.; Jia, Y.; Yu, X.; Mou, R.; Li, X. Hispidulin Inhibits Proliferation, Migration, and Invasion by Promoting Autophagy via Regulation of PPARγ Activation in Prostate Cancer Cells and Xenograft Models. *Biosci. Biotechnol. Biochem.* **2021**, *85*, 786–797. [CrossRef]
66. Sun, Y.; Duan, X.; Wang, F.; Tan, H.; Hu, J.; Bai, W.; Wang, X.; Wang, B.; Hu, J. Inhibitory Effects of Flavonoids on Glucose Transporter 1 (GLUT1): From Library Screening to Biological Evaluation to Structure-Activity Relationship. *Toxicology* **2023**, *488*, 153475. [CrossRef] [PubMed]
67. Chang, C.-J.; Hung, Y.-L.; Chen, T.-C.; Li, H.-J.; Lo, Y.-H.; Wu, N.-L.; Chang, D.-C.; Hung, C.-F. Anti-Proliferative and Anti-Migratory Activities of Hispidulin on Human Melanoma A2058 Cells. *Biomolecules* **2021**, *11*, 1039. [CrossRef]
68. Kim, H.A.; Lee, J. Hispidulin Modulates Epithelial-Mesenchymal Transition in Breast Cancer Cells. *Oncol. Lett.* **2021**, *21*, 155. [CrossRef] [PubMed]